Improved Kriging-Based Approach for the Probabilistic Analysis of a Large Diameter Monopile in a Spatially Varying Soil

Abdul Kader El Haj[1] and Abdul-Hamid Soubra[2]

[1]University of Nantes, Bd. de l'Université, 44603 Saint-Nazaire Cedex, France.
E-mail: abdul-kader.el-haj@univ-nantes.fr
[2]University of Nantes, Bd. de l'Université, 44603 Saint-Nazaire Cedex, France.
E-mail: abed.soubra@univ-nantes.fr

Abstract: In this paper, a probabilistic analysis of an offshore monopile foundation embedded in a spatially varying clayey soil was performed. An efficient Kriging-based probabilistic approach using a multipoint enrichment was adopted. The aim is to compute the failure probability P_f against exceeding a threshold value on the monopile head rotation. The proposed probabilistic approach was shown to significantly reduce the computation time with respect to the classical Kriging-based approach. Some probabilistic numerical results are presented and discussed.

Keywords: Probabilistic analysis; monopile foundation; spatial variability; failure probability; Kriging.

1 Introduction

Recently, a Kriging-based probabilistic technique was proposed by Al-bittar et al. (2018) to compute the small values of the failure probability of geotechnical structures involving spatially varying soils. This technique (called AK-MCS) is an Active learning method combining Kriging with Monte Carlo Simulation MCS method. Other active learning methods may be found in literature as the active learning method by Huang et al. (2016) that combines Kriging and Subset Simulation and the global sensitivity analysis-enhanced surrogate (GSAS) modeling suggested by Hu and Mahadevan (2016). Although the AK-MCS method has been proved to require a reduced number of calls to the mechanical model with respect to the variance reduction techniques such as Subset Simulation SS and Asymptotic Sampling AS, it remains time-consuming in the case of costly-to-evaluate mechanical models such as the three-dimensional mechanical model considered in this paper.
In order to reduce the computation time, an improved probabilistic model is suggested in this paper. This model is an extension of the AK-MCS approach in which a multipoint enrichment technique is used. It is called AK-MCSm (where m stands for multi-enrichment). A relevant clustering technique [see Lelièvre et al. (2018)] was adopted. This technique allows one to consider a set of training samples that ensures a suitable coverage of the limit state surface.

In this paper, one performs a probabilistic analysis at the ultimate limit state (ULS) of a monopile foundation embedded in a spatially varying soil making use of the relevant multi-enrichment approach AK-MCSm. The aim is to compute the failure probability P_f against exceeding a threshold value on the monopile head rotation.

2 Soil-Monopile Mechanical Model

The mechanical model of the 3D soil-monopile system has been carried out based on numerical simulations using the commercial finite element software Abaqus (2016). An open-ended steel monopile of diameter D=4m was studied in this paper. The monopile of 0.05 m thickness and an embedment depth L of 24 m was extended of 1.0 m above the seabed to avoid the soil from going over the monopile. The steel monopile has a density of 7840 $\mathrm{kg/m^3}$. It was assumed to behave as a linear elastic material with Young modulus E_p of 210 GPa and Poisson ratio ν_p of 0.3.

The soil consists of an undrained normally consolidated clay. It was supposed to follow an elastic-perfectly plastic model based on Tresca criterion. This model is defined by the undrained cohesion c_u, the undrained Young modulus (E_u) and the undrained Poisson ratio (ν_u). In this paper, the soil was assumed to have a submerged unit weight of 7 $\mathrm{kN/m^3}$ and an undrained Poisson ratio of 0.495. The undrained cohesion was supposed to linearly vary with depth as follows:

$$c_u = 2 + 0.24\,\sigma'_{v0} \qquad [kPa] \tag{1}$$

where σ'_{v0} is the effective vertical overburden stress. This represents an increase in c_u from its initial value at mudline (taken here equal to 2 kPa) at a rate of about 1.68 kPa/m. These adopted values are typical for a

Proceedings of the 7th International Symposium on Geotechnical Safety and Risk (ISGSR)
Editors: Jianye Ching, Dian-Qing Li and Jie Zhang

Published by Research Publishing, Singapore.
ISBN: 978-981-11-2725-0; doi:10.3850/978-981-11-2725-0_IS9-4-cd

normally consolidated offshore clay [cf. Dean (2010)]. Notice that the soil undrained Young modulus was assumed to be linearly related to the soil undrained cohesion *via* the relationship $E_u = K_c \times c_u$ where K_c is a correlation factor that is dependent on the clay plasticity index PI and the over-consolidation ratio OCR [cf. USACE (1990)]. Thus, the soil Young modulus was also supposed to linearly vary with depth. For a plasticity index $PI = 35\%$ and an over-consolidation ratio of 1, a value of $K_c = 500$ is adopted in this work [cf. USACE (1990)].

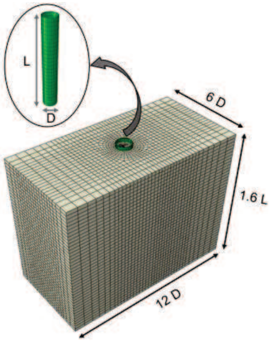

(a)

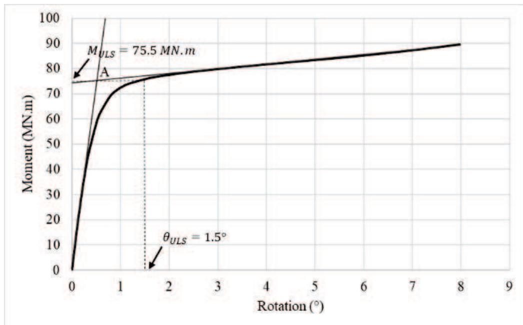

(b)

Figure 1. (a) Three-dimensional soil-monopile numerical model (b) Moment-rotation curve of the monopile at mud-line level.

As may be seen from Figure 1(a), the numerical model has a length of 12D, a width of 6D and a height of 1.6 L. Details on the numerical modeling of the soil-monopile system are not provided herein. The reader may refer to El Haj et al. (2019).

In this paper, the monopile was considered to be subjected to a horizontal load $H = 1.6\ MN$ acting at a height h=38.6m above the seabed level. This results in an additional moment at mudline of $M = 61.7\ MN.m$. A vertical load V of 2 MN that represents the structure weight was also considered in the analysis. The applied loadings adopted in this study induced a head rotation at mudline (as computed by Abaqus software) of nearly 0.55°.

Concerning the determination of the ultimate rotation at the monopile head, a load-controlled procedure was used. The corresponding moment-rotation curve is shown in Figure 1(b). As it may be seen from this figure, the ultimate rotation was determined by the tangent intersection method (point A) leading to a limit rotation of $\theta_{ULS} = 1.5°$ and a corresponding ultimate moment capacity at mudline of $M_{ULS} = 75.5\ MN.m$. This corresponds to an ultimate horizontal force of $1.95\ MN$. The obtained ultimate value of the monopile head rotation will be used afterwards in this paper as a threshold value when handling the probabilistic analysis.

3 Probabilistic Model

The soil undrained cohesion c_u was considered as a log-normal random field with a constant coefficient of variation of 25%. The mean values of the soil undrained cohesion are those of the deterministic analysis provided in the preceding section. Concerning the autocorrelation function, a square exponential function $\rho_Z^{LN}(X, X')$ was used in this paper. The soil undrained Young modulus was implicitly considered as a random field having the same distribution as the soil undrained cohesion since it was assumed to be linearly related to the soil cohesion.

Notice that the discretization of the cohesion random field was performed using EOLE method proposed by Li and Der Kiureghian (1993). Notice also that the discretization of a random field by EOLE leads to an expression that provides the value of this random field at each point of the soil mass as a function of M standard Gaussian random variables (this number M is equal to the number of eigenmodes). Notice finally that the realizations of the Young modulus random field can be easily obtained from the realizations of the cohesion random field by multiplying the values of the soil cohesion by 500.

The probabilistic analysis at ULS aims at computing the failure probability P_f against exceeding a threshold value on the ultimate rotation of the monopile head. The performance function is given by:

$$G = \frac{\theta_{ULS}}{\theta} - 1 \qquad (2)$$

where θ_{ULS} is the ultimate rotation of the monopile head as was determined before using the mean values of E_u and c_u ($\theta_{ULS} = 1.5°$) and θ is the monopile head rotation under the applied loading for typical realizations of c_u and E_u. The computation time of θ for each simulation *via* Abaqus software was equal to about one hour.

The AK-MCSm probabilistic method used in this paper is based on Kriging metamodeling. Notice that the Kriging consists in constructing a meta-model based on a few number of samples (called Design of Experiment DoE) computed using the mechanical model. The predicted response at an unknown sample (based on the constructed Kriging meta-model) is a Gaussian random variate characterized by a mean prediction value and a corresponding prediction variance. The construction of a Kriging metamodel can be easily performed using DACE (Design and Analysis of Computer Experiments) toolbox in Matlab. For more details, the reader may refer to Lophaven et al. (2002). The present probabilistic AK-MCSm procedure consists of two main stages. These two stages may be described as follows:

3.1 Construction of a preliminary Kriging metamodel

In this stage, one first generates a MCS population of 5×10^5 samples $\boldsymbol{x}^{(i)}(i = 1,2, \ldots, 5 \times 10^5)$. Each sample $\boldsymbol{x}^{(i)}$ is a vector of *M* standard Gaussian random variables where *M* is the number of random variables required by EOLE methodology to accurately discretize the random field. Secondly, a small design of experiment DoE (taken equal to 15 samples) is randomly selected from the generated population. Each sample of the DoE is transformed (using EOLE) into a realization of c_u and a corresponding realization of E_u using $E_u = 500 \times c_u$. These realizations are used as inputs for the mechanical model while computing the sample system response (i.e. monopile head rotation θ) and the corresponding performance function value.

By using the DACE toolbox [cf. Lophaven et al. (2002)], an approximate Kriging meta-model may be constructed in the standard space of random variables on the basis of the DoE and the corresponding performance function values. This meta-model may be used to compute the MCS failure probability P_f and its corresponding coefficient of variation $COV(P_f)$. It should be noted that the value of P_f and the corresponding value of $COV(P_f)$ computed so far are not sufficiently accurate. This is because of the very small number of samples (i.e. small size of the DoE) used to construct the present preliminary Kriging metamodel. Thus, an enrichment process is needed.

3.2 Enrichment process

The enrichment process is done *via* an active learning technique. The learning phase stops once the metamodel becomes sufficiently accurate for the computation of the failure probability, which is indicated by a stopping criterion. The aim of the next two subsections is to present the way of selection of the new training samples during the enrichment process and the adopted stopping criterion.

3.2.1 Selection of new training samples

The enrichment process of the AK-MCS method is performed using a learning function U defined by the following equation [see Echard et al. (2011)]:

$$U\left(x^{(i)}\right) = \frac{|\hat{g}(x^{(i)})|}{\sigma_{G_p}(x^{(i)})} \tag{3}$$

where σ_{G_p} is the square root of the Kriging prediction variance. The sample that has the minimum value of U is selected for the enrichment since it is considered to have the highest probability of being misclassified (i.e. the highest probability to have a wrong performance function sign) as was stated by Echard et al. (2011). It should be remembered that AK-MCS method involves a single sample per iteration of the enrichment process. In order to overcome this shortcoming, a multipoint enrichment procedure is adopted in this paper.

Lelièvre et al. (2018) proposed a clustering technique, named K-weighted-means clustering algorithm (K-w-means), that takes benefit of the information provided by the AK-MCS learning function. The K-w-means technique consists in replacing the mean of each cluster by a weighted one making use of the learning function *U*. In this way, each sample will be weighted by the corresponding uncertainty of being misclassified (i.e. the uncertainty to have a wrong sign of its performance function) and thus, the obtained centroids of the different clusters will be the optimal ones for the enrichment. In other words, the selected samples will be situated in the highly uncertain zone (i.e. the zone corresponding to a high uncertainty on the sign of the performance function) all along the limit state surface leading to an efficient multipoint enrichment of the Kriging meta-model. This approach is used in this paper. For more details, the reader may refer to El Haj and Soubra (2019).

3.2.2 Stopping condition

In AK-MCS method, the stopping condition is defined from the perspective of individual responses (not the quantity of interest P_f), which may lead to some unnecessary extra evaluations of the mechanical model. A more relevant stopping condition that is based on the convergence of the quantity of interest (i.e. P_f) was proposed by

Schöbi et al. (2017). This criterion was used in this paper in the aim to reduce the computation time. Indeed, the adopted criterion relies on the convergence of the failure probability, which could be attained before reaching the stopping condition indicated by AK-MCS.

Schöbi et al. (2017) define a limit state margin characterized by upper and lower boundaries of the limit state surface that takes into account the prediction uncertainty in the Kriging metamodel. These authors stated that when these boundaries become close to each other, a thin limit state margin is obtained and thus, the estimated failure probability can be considered as accurate. The proposed stopping criterion is given as follows:

$$\varepsilon_{P_f} = \frac{P_f^+ - P_f^-}{P_f^0} \leq \varepsilon_t \tag{4}$$

where P_f^0 is the original failure probability based on the Kriging prediction values $P(\hat{g}(x) \leq 0)$ and, P_f^+ and P_f^- are respectively the upper and lower boundaries of the failure probability defined as follows:

$$P_f^+ = P[(\hat{g}(x) + t.\sigma_{G_p}(x)) \leq 0] \tag{5}$$

$$P_f^- = P[(\hat{g}(x) - t.\sigma_{G_p}(x)) \leq 0] \tag{6}$$

where $\hat{g}(x) + t.\sigma_{G_p}(x) = 0$ and $\hat{g}(x) - t.\sigma_{G_p}(x) = 0$ are respectively the upper and lower boundaries of the limit state surface defined by $\hat{g}(x) = 0$, t is a constant ($t = 2$ in this paper) that sets the confidence level equal to $2 = \Phi^{-1}(97.7\%)$ and ε_t is a given tolerance taken as $\varepsilon_t = 10\%$ in this paper.

4 Probabilistic Numerical Results

A reference case where the vertical autocorrelation distance was taken equal to 2m was considered, the soil being assumed to be homogeneous in the horizontal direction. The number of random variables required by EOLE to accurately discretize the random field with a small variance of error (<5%) was found equal to 20. This number of random variables was adopted in the present paper.

Table 1. Results of AK-MCS and AK-MCSm approaches.

Method	$P_f \times 10^{-3}$	Number of added samples	Time (days)
AK-MCS	1.274	447	27.89
AK-MCSm (4 clusters)	1.274	520	7.28

Table 1 presents the results of AK-MCS approach and those of the proposed AK-MCSm method. As may be seen from this table, the two approaches result in the same value of the failure probability. Concerning the computation cost, the proposed method leads to a significant reduction in the computation time as compared to AK-MCS (7.28 days for AK-MCSm instead of 27.89 days for AK-MCS).

4.1 Effect of the autocorrelation distances a_x, a_y and a_z on P_f

Figure 2 presents the evolution of the failure probability with a_x, a_y and a_z where a_x and a_y are the horizontal autocorrelation distances in the directions orthogonal and parallel to the loading plane respectively and a_z is the vertical autocorrelation distance. The aim of this figure is to identify (for the present embedded length and diameter of the monopile) the values of the autocorrelation distances for which the soil spatial variability has a significant effect on the computed failure probability.

For all the three curves of Figure 2, the failure probability increases with the different autocorrelation distances a_x, a_y or a_z. The rates of increase of the failure probability largely decrease beyond given values of the autocorrelation distances [i.e. beyond an autocorrelation distance of 24m (≈L) for a_z, 10m (≈2.5D) for a_y and 6m (≈1.5D) for a_x] to attain a constant value of the failure probability corresponding to the case of a homogeneous soil (i.e. with no spatial variability). The failure probability corresponding to the homogeneous case was found equal to 0.12. It should be emphasized here that all the three identified distances (i.e., L, 2.5D and 1.5D) are directly related to the soil displacement field obtained due to the ultimate loading (i.e. they are related to the mechanics of the problem and not connected to the input probabilistic data). Indeed, the deformed soil at the ultimate limit state (i.e. at the ultimate rotation) is concentrated along the embedded length L of the monopile in the vertical direction, and it is limited to 2.5D and 1.5D in the y- and x- horizontal directions as it may be seen from Figures 3(a) and 3(b), respectively. These observations explain the reason why the increase in the autocorrelation distances a_x, a_y and a_z beyond the distances 1.5D, 2.5D and L respectively does not significantly change the value of the failure probability. A reduction in the failure probability with respect to the case of a homogeneous soil may be obtained if at least one of the autocorrelation distances a_x, a_y or a_z is smaller than its corresponding limit value (i.e. 1.5D, 2.5D, L) since the monopile head rotation will be affected by the soil spatial variability in this case, thus inducing a change in the failure probability.

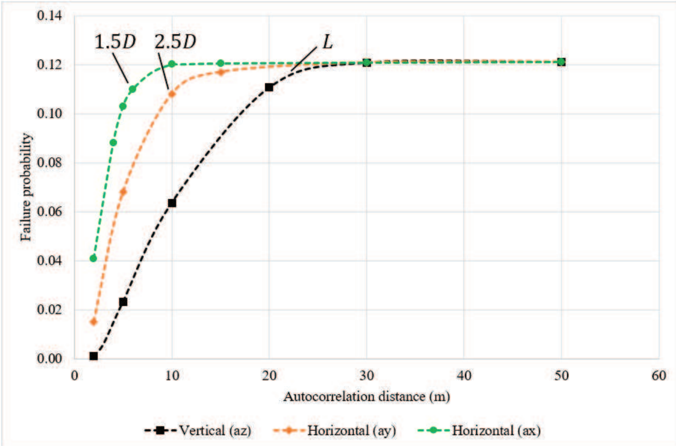

Figure 2. Effect of the autocorrelation distances a_x, a_y and a_z on P_f.

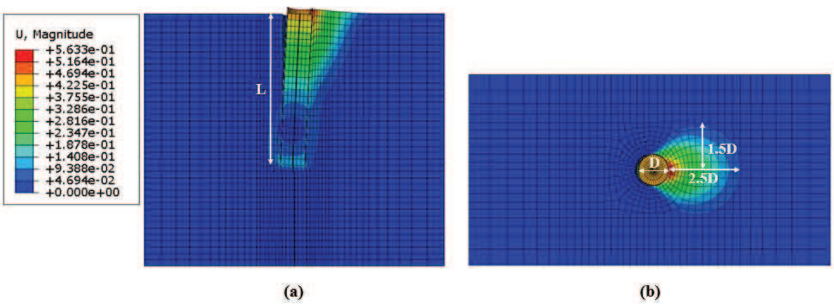

Figure 3. Deformed soil at the ultimate limit state (a) in the yz plane (b) in the xy plane.

Figure 2 shows that the rate of increase in the failure probability (for the small and moderate values of the autocorrelation distances) is the highest when considering the horizontal autocorrelation distance a_x. This rate of increase in the failure probability is smaller for the horizontal autocorrelation length a_y and it becomes the smallest one for the vertical autocorrelation distance a_z. These observations indicate that a significant reduction in the failure probability with respect to the one corresponding to the homogeneous case, may be obtained by first considering the spatial variability in the vertical direction; the spatial variability in the horizontal direction(s) although important could be considered in a second stage. This result is interesting especially that the identification of the soil spatial variability in the vertical direction is easier and cheaper (e.g. by using a CPT test).

5 Conclusions

A probabilistic analysis at the ultimate limit state (ULS) was performed in this paper for an offshore monopile foundation embedded in a spatially varying clayey soil. A Kriging-based probabilistic approach using a multipoint enrichment technique was adopted. An improved clustering technique proposed by Lelièvre et al. (2018) was used for learning. Also, this paper makes use of a relevant stopping condition recently proposed by Schöbi et al. (2017). The method was shown to be efficient in terms of the computation time with respect to AK-MCS approach. A reduction in the failure probability with respect to the case of a homogeneous soil may be obtained if at least one of the autocorrelation distances a_x, a_y or a_z is smaller than its corresponding limit value (i.e. 1.5D, 2.5D, L).

Acknowledgments

This work was carried out within the framework of the WEAMEC, WEst Atlantic Marine Energy Community, and with funding from the CARENE, Communauté d'Agglomération de la Région Nazairienne et de l'Estuaire.

References

Abaqus (2016). *Dassault Systèmes Simulia Corp, Providence.*

Al-Bittar, T., Soubra, A.-H., and Thajeel, J. (2018). Kriging-based reliability analysis of strip footings resting on spatially varying soils. *Journal of Geotechnical and Geoenvironmental Engineering*, 144(10).

Dean, E.T.R. (2010). *Offshore Geotechnical Engineering: Principles and Practice*, Thomas Telford, London.

Echard, B., Gayton, N., and Lemaire, M. (2011). AK-MCS: An active learning reliability method combining Kriging and Monte Carlo Simulation. *Structural Safety*, 33(2), 145–154.

El Haj, A.-K., and Soubra, A.-H. (2019). Application of improved Kriging-based approaches to the analysis of monopile foundations. *13th International Conference on Applications of Statistics and Probability in Civil Engineering ICASP13*, Seoul, South Korea, May 26-30.

El Haj, A.-K., Soubra, A.-H., and Fajoui, J. (2019). Probabilistic analysis of an offshore monopile foundation taking into account the soil spatial variability. *Computers and Geotechnics*, Elsevier, 106, 205–216.

Hu, Z. and Mahadevan, S. (2016). Global sensitivity analysis-enhanced surrogate (GSAS) modeling for reliability analysis. *Structural and Multidisciplinary Optimization*, 53(3), 501–521.

Huang, X., Chen, J., and Zhu, H. (2016). Assessing small failure probabilities by AK–SS: An active learning method combining Kriging and Subset Simulation. *Structural Safety*, 59, 86–95.

Lelièvre, N., Beaurepaire, P., Mattrand, C., and Gayton, N. (2018). AK-MCSi : A Kriging-based method to deal with small failure probabilities and time-consuming models. *Structural Safety*, 73, 1–11.

Li, C.-C. and Der Kiureghian, A. (1993). Optimal discretization of random fields. *Journal of Engineering Mechanics*, 119(6), 1136–1154.

Lophaven, S.N., Nielsen, H.B., and Søndergaard, J. (2002). *DACE: A Matlab Kriging Toolbox Version 2.0*, Informatics and Mathematical Modelling, Technical report IMM-TR-2002-12, Technical University of Denmark, DTU.

Schöbi, R., Sudret, B., and Marelli, S. (2017). Rare event estimation using Polynomial-Chaos Kriging. *ASCE-ASME Journal of Risk and Uncertainty in Engineering Systems, Part A: Civil Engineering*, 3(2), 1–12.

USACE (1990). *Engineering and Design : Settlement Analysis*, Engineer Manual 1110–1–1904, US Army Corps of Engineers.